Role of Electronegative Atom Present on Ligand Backbone and Substrate Binding Mode on Catecholase- and Phosphatase-Like Activities of Dinuclear Ni II Complexes: A Theoretical Suppo…

Article *in* ChemistrySelect · February 2018

DOI: 10.1002/slct.201702861

CITATION
1

READS
158

6 authors, including:

Jaydeep Adhikary
Ariel University
35 PUBLICATIONS **375** CITATIONS
SEE PROFILE

Ishani Majumder
University of Calcutta
15 PUBLICATIONS **70** CITATIONS
SEE PROFILE

Priyanka Kundu
University of Calcutta
7 PUBLICATIONS **65** CITATIONS
SEE PROFILE

Haya Kornweitz
Ariel University
42 PUBLICATIONS **555** CITATIONS
SEE PROFILE

ChemPubSoc Europe

DOI: 10.1002/slct.201702861

Chemistry SELECT Full Papers

Inorganic Chemistry

Role of Electronegative Atom Present on Ligand Backbone and Substrate Binding Mode on Catecholase- and Phosphatase-Like Activities of Dinuclear Ni^{II} Complexes: A Theoretical Support

Jaydeep Adhikary,*[a, b] Ishani Majumdar,[b] Priyanka Kundu,[b] Haya Kornweitz,[a] Hulya Kara,[c, d] and Debasis Das*[b]

The reaction of two pentadentate compartmental ligands HL^1 and HL^2 [HL^1 = 2,6-bis((*E*)-(2-morpholinoethylimino)methyl)-4-*tert*-butylphenol; HL^2 = 2,6-bis((*E*)-(2-(piperidin-1-yl)ethylimino) methyl)-4-*tert*-butylphenol] with nickel acetate followed by addition of NaSCN afforded two discrete dinuclear complexes, $[Ni_2L^1(CH_3COO)_2(SCN)]\cdot(H_2O)_2\cdot(0.5CH_3OH)$ (**1**) and $[Ni_2L^2(CH_3COO)(SCN)_2(CH_3OH)]\cdot(CH_3OH)$ (**2**). Single crystal structure reveals that the complexes are Ni^{II} dimer with triple-mixed phenoxo and acetate/isothiocyanate bridges. Variable-temperature (3-300 K) magnetic studies have been performed and data analyses reveal that the dinuclear nickel(II) units show a weak ferromagnetic coupling in complex **1** ($J = +3.70$) and a weak antiferromagnetic coupling in complex **2** ($J = -0.87\ cm^{-1}$). The catalytic promiscuity of the complexes in terms of two different bio-relevant catalytic activities like oxidation (catecholase) and hydroxylation (phosphatase) has been thoroughly explored. Role of an auxiliary electronegative atom present on the ligand backbone and binding approach of the substrate to the metal centres during the catalytic activities have been scrutinized by DFT calculation. Several experimental techniques have been utilised to evaluate the mechanistic interpretation of catecholase like activity. And finally, mechanistic pathway of both the bio activities are demonstrated.

Introduction

During the last few years, much of the information regarding the role of metals in dinuclear oxidative and hydrolytic metalloenzymes, such as catechol oxidases and phosphatases is gained through comparative studies on metalloenzymes and synthetic model metal complexes.[1] Studies with model complexes have been described, aiming to mimic the structural and/or functional properties of these metalloenzymes, such as the intermetallic distance,[2] asymmetry,[3] and geometry around each metal center,[4] with the presence of labile sites essential for binding of the substrate and/or available nucleophiles to initiate the catalytic process.[5]

Our laboratory has been actively engaged to access the mechanistic pathway of catechol oxidase as well as phosphatase activity for the last few years. We have recently reported the role of solvent in catecholase and phosphates like activities.[6] We have also succeeded to expose the role of the para substituent group present in the end-off ligand on these bio mimicking studies.[7] In those cases, we took phenolic aldehyde with different substitution on their para position to -OH group and followed by the condensation with amine to prepare the ligand. The ligands having different substitution on the para position were considered for the preparation of metal complexes and followed by the study on their catecholase and phosphatase like activity. Very recently we have explored the effect of Lewis acidity of group 12 metal on phosphatase like activity.[8] However, the role of auxiliary electronegative atom present in the amine part was not investigated over these catalytic processes. Our group has recently investigated the effect auxiliary atoms[9] in overall coordination chemistry in terms of structural and solid-state phenomenon but the effect on catalytic efficiencies have not been yet explored. These deficiencies therefore motivated us towards our current investigation. Consequently, in the present project two Ni^{II} complexes, namely, $[Ni_2L^1(CH_3COO)_2(SCN)]\cdot(H_2O)_2\cdot(0.5CH_3OH)$ (**1**) and $[Ni_2L^2(CH_3COO)(SCN)_2(CH_3OH)]\cdot(CH_3OH)$ (**2**) have been syn-

[a] *Dr. J. Adhikary, Prof. H. Kornweitz*
Department of Chemical Sciences
Ariel University
Ariel 40700, Israel
E-mail: adhikaryj86@gmail.com
[b] *Dr. J. Adhikary, I. Majumdar, Dr. P. Kundu, Prof. D. Das*
Department of Chemistry
University of Calcutta
92, A. P. C. Road, Kolkata – 700009, India
E-mail: dasdebasis2001@yahoo.com
[c] *Prof. H. Kara*
Department of Physics
Faculty of Science and Art
Balikesir University
Balikesir, Turkey
[d] *Prof. H. Kara*
Department of Physics
Faculty of Science
Mugla Sıtkı Koçman University
Mugla, Turkey

Supporting information for this article is available on the WWW under https://doi.org/10.1002/slct.201702861

thesised with only difference in an auxiliary atom present in the amine moiety, *i:e* HL^1 has two oxygen atoms whereas HL^2 contain carbon atoms (more specifically -CH_2- group) in the same position (Scheme 1). Analogous nickel complex with

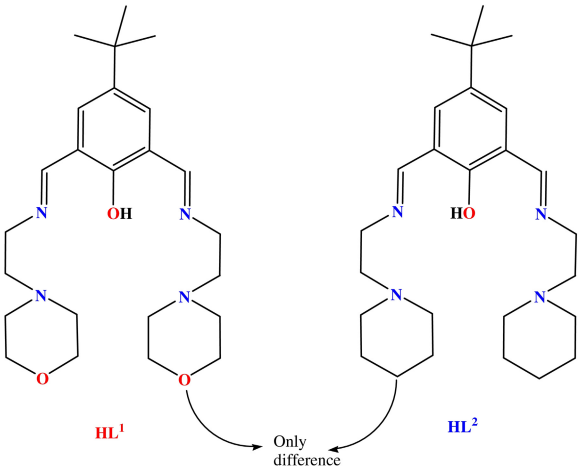

Scheme 1. End off compartmental ligands HL^1 and HL^2.

nitrogen atom as the auxiliary atom could not be incorporated in this report as the nitrogen atom become protonated during complexation, causing remarkable enhancement of catecholase activity, reported earlier by our group.[10]

Herein, the catecholase and phosphatase like activity have been inspected using 3,5-di-*tert*-butylcatechol (3,5-DTBC) and 4-nitrophenylphosphate (4-NPP), as a model substrate, respectively, to evaluate the role of the auxiliary atoms in these catalytic promiscuities. The present study reveals that complex **1** shows higher activity towards both the bio activities. DFT calculations have been performed to rationalize the experimental observation. Combined experimental and theoretical investigations help us to explore new findings in the study on catecholase like activity of dinuclear Ni^{II} complexes and all those findings have been well documented in this manuscript.

Along with the unique catalytic behavior an interesting magnetic behavior have also been explored here. The magnetic study shows that different behavior within the Ni^{II} dimers (a weak ferromagnetic coupling in complex **1** and a weak antiferromagnetic coupling in complex **2,** due to the different bridges between Ni^{II} centres and changes in the coordination geometries). To the best of our knowledge, complex **1** is the first report and complex **2** is the second report of a Ni^{II} dimer containing triple-mixed μ-phenoxo, μ_2-η^2:η^1 acetate/end-on isothiocyanate and μ_2-1,3 *syn-syn* acetate bridges which have been structurally and magnetically characterized.

Results and discussions

Syntheses and characterization

The Schiff-base ligands, HL^1 and HL^2, were synthesized through the classical condensation reaction of 2,6-diformyl-*tert*-butylphenol with N-(2-aminoethyl)morpholine and N-(2-aminoethyl) piperidine respectively, in methanol medium. The Schiff-base ligands on treatment with nickel (II) acetate followed by addition of NaSCN produced complexes **1** and **2**. Both the complexes show FTIR bands due to C=N stretch in the range around ~1654 cm^{-1} and skeletal vibration in the range 1575–1578 cm^{-1}(**Figure S1–S2**). One FTIR stretching at 2089 cm^{-1} for **1** indicates the presence of thiocyanate ligand with single mode of binding whereas in complex **2** two bands at 2019 and 2095 cm^{-1} suggest two different binding modes of thiocyanate ligands that is also supported by crystal structure analysis. Both the complexes exhibit one strong IR peak around ~1420 cm^{-1} due to presence of acetate molecule. 10^{-2} M methanolic solutions of two complexes show four d-d bands in their electronic spectra (UV-Vis-NIR region), suggesting octahedral coordination environment around both nickel (II) centers (**Figure S3**). The transition at ~1207 nm, ~917-870 nm, ~600 nm and ~375 nm can be assigned as $^3A_{2g}$-$^3T_{2g}$(F), $^3A_{2g}$-$^3T_{1g}$(F), $^3A_{2g}$-$^1E_{1g}$ and $^3A_{2g}$-$^3T_{1g}$(P) respectively as reported earlier.[11]

Description of crystal structures

The ORTEP diagrams of complexes **1** and **2** are depicted in Figure 1-2. Selected bond lengths and angles for complexes **1**

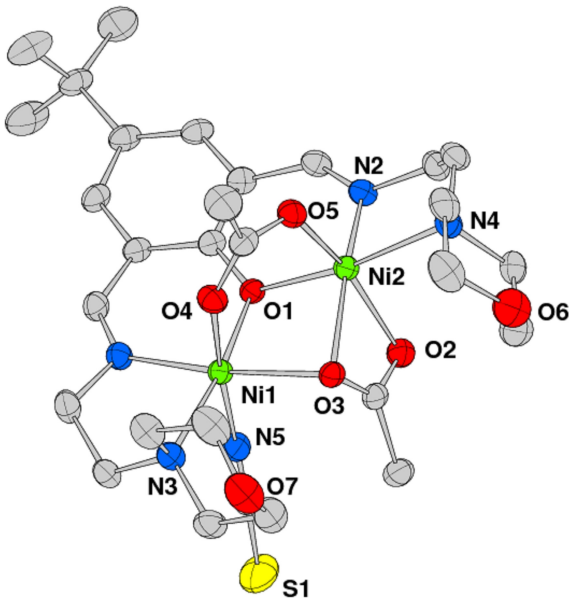

Figure 1. Molecular structure of complex **1** (ORTEP drawing, ellipsoid probability 35%). Lattice solvent molecules not shown here. Hydrogens are omitted for clarity.

and **2** are tabulated in **Table S1** and **S2**, respectively. Both thiocyanate derivates **1** and **2** are discrete dinuclear complex. The X-ray crystallography confirms that two nickel ions are bridged by the pentadentate ligand L^1 or L^2 acting through phenolic oxygen in addition to the imine and the morpholine nitrogen donors (L^1) or piperidine nitrogens (L^2). In each case the coordination sphere of the metal is a distorted octahedron.

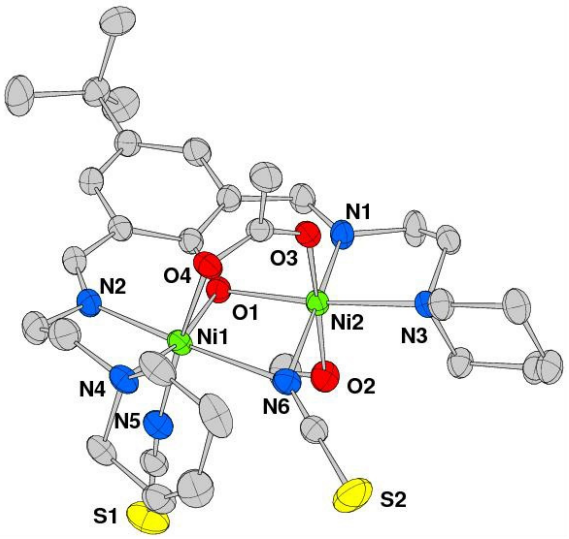

Figure 2. Molecular structure of complex **2** (ORTEP drawing, ellipsoid probability 35%). Lattice methanol molecule not shown here. Hydrogens are omitted for clarity.

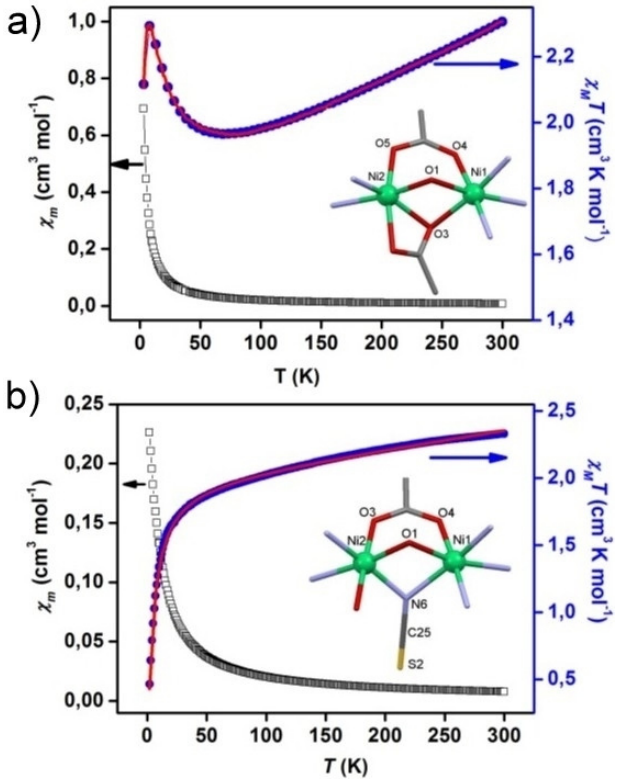

Figure 3. Temperature dependence of χ_M and $\chi_M T$ per Ni_2 for **1** (a) and **2** (b). The solid red line represents the best-fit obtained using Eq. 2. (inset-the magnetic exchange coupling pathway for complex **1** and **2**).

In the former species, the sole isothiocyanate occupies an axial position at Ni1. Although, in **2** two SCN species behave as bridging and monodentate ligand. It is of interest that in **1**, one acetate anion assumes the usual μ_2 −1,3 *syn-syn* bridging mode, while the other is μ_2-η^2:η^1. The latter coordination mode is less frequent[12] leading to longer Ni–O bond distances (range 2.157(2)-2.146(3) Å) those involving the *syn-syn* bridging acetate (2.052(3) and 1.998(3) Å, **Table S1**. In complex **2**, one acetate ligand is bridging between two metal centres in *syn-syn* μ-bridging mode. The Sixth coordination of Ni2 centre of complex **2** is satisfied by one methanol molecule. Here the metal chromophores in the two complexes are different, being N_3O_3/N_2O_4 and N_4O_2/N_3O_3, respectively. In complex **1** the bond angles Ni1-O1-Ni2 and Ni1-O3-Ni2 are 97.53° and 91.03°, respectively. Phenoxy bridged bond angles Ni1-O1-Ni2 for complex **2** is 97.43°, slightly lower in compare to **1**. Another bridging angle Ni1-N6-Ni2 is 89.05°. Surprisingly, the intermetallic Ni1-Ni2 distances in **1** and **2** are very comparable having ~3.071 Å though the environment around both nickel centres in two complexes are different.

In addition, the complexes are connected by O–H…O, O–H…S, C–H…O and C–H…S weak hydrogen bonding network (**Figure S4–S7**). This hydrogen bonded networks lie in the *ab*-plane and stacks along to the c-axis (**Figure S5** and **S7**). The short intermolecular Ni^{II}… Ni^{II} distances are 6.382 for complex **1** and 8.220 for complex **2** in packing structures.

Magnetic properties of the complexes 1–2

The magnetic properties of **1** and **2**, in the form of χ_M and $\chi_M T$ (χ_M is the susceptibility per dimeric unit) *vs.* T plots, are shown in Figure 3 in a temperature range 3–300 K. The $\chi_M T$ value at room temperature, 2.30 cm^3 K mol^{-1} ($\mu_{eff=}$ 4.29 μ_B) for **1** and 2.33 emu K mol^{-1} ($\mu_{eff=}$ 4.31 μ_B) for **2**, which are a little higher than the expected value of 2 emu K mol^{-1} (μ_{eff} =4 μ_B) of two independent Ni^{II} ions ($S=1$ with $g=2.0$), which agrees with the value found for similar compounds,[13,14] which is mainly due to the orbital contribution of the Ni^{II} ions. When decreasing the temperature, the $\chi_M T$ product decreases gradually to a minimum at 70 K and then rises to a maximum of 2.29 emu K mol^{-1} at 8 K and final decrease to 2.10 emu K mol^{-1}at 3 K for **1**, suggesting the presence of a ferromagnetic interaction between the pair of nickel(II) ions. In case of **2**, the $\chi_M T$ value decreases monotonously to a minimum of 0.46 emu K mol^{-1} at 3 K, evidently an antiferromagnetic interaction operates between the pair of nickel ions. The decrease in $\chi_M T$ at low temperatures is more likely due to zero-field splitting effects (ZFS) of the ground state and/or possible intermolecular interactions between the dimers.[15]

The experimental magnetic susceptibility data have been analyzed using the isotropic spin Hamiltonian $H=-2JS_1S_2$ for spin coupled dinuclear with $S_1=S_2=1$ as shown in Eq. (1),[14] where $x=J/kT$. In addition, the inter-dimer exchange interaction was taken into account by using the mean field approximation Eq. (2).[16,17]

$$\chi_{dimer}T = \frac{2Ng^2\mu_B^2}{k}\frac{e^{2J/kT}+5e^{6J/kT}}{1+3e^{2J/kT}+5e^{6J/kT}} + N_\alpha \qquad (1)$$

Table 1. Selected structural and magnetic data for complexes **1–2**.

Complex	bridging moiety	Ni-Ni (Å)	Ni-O-Ni (°)	Ni-X-Ni (°)	Ni(1)–O–X–Ni(2) (°)	δ (°)	J (cm^{-1})	J′ (cm^{-1})
1	μ-phenoxido–μ_2-η_2:η_1 acetate–μ_2 −1,3 syn-syn acetate	3.070	97.53	91.03	19.19	25.18	+3.70	- 0.10
2	μ-phenoxido–$\mu_{1,1}$-isothiocyanate–μ_2 −1,3 syn-syn acetate	3.071	97.43	89.05	15.45	23.74	- 0.87	- 0.77

X : μ_2-η_2:η_1 acetate (**1**) and $\mu_{1,1}$-isothiocyanate (**2**)

$$\chi_M T = \frac{\chi_{dimer} T}{1 - \chi_{dimer}(2zJ'/Ng^2\beta^2)} \quad (2)$$

Where χ_M denotes the magnetic susceptibility per dinickel (II), J is the intra-dimer exchange parameter, zJ' is the inter-dimer exchange parameter, z is the number of nearest neighbours of each dimer (z = 2, as in **1** and **2**), N_α is the temperature-independent paramagnetism and the other symbols have their usual meaning. The best fitting of the least-square analysis of magnetic data with the Eq. (2) leads to $J = +3.70\ cm^{-1}$, $J' = -0.1\ cm^{-1}$, $N_\alpha = 0.000198$, $g = 2.14$ for **1** ($R^2 = 0.9992$) and $J = -0.87\ cm^{-1}$, $J' = -0.77\ cm^{-1}$, $N_\alpha = 0.000193$, $g = 2.16$ for **2** ($R^2 = 0.99758$).

In addition to some relevant structural information, the *J* values of **1** and **2** are listed in Table 1. The difference in the exchange couplings constant can be explained by structural differences in **1** and **2**. There are three magnetic exchange pathways because of the occupation of μ-phenoxo and μ_2-η_2:η_1 acetate (for **1**) / end-on isothiocyanate (for **2**) bridges in the equatorial positions, as well as μ_2-1,3 *syn-syn* acetate bridge in the axial positions (see Figure 3 (inset)). It is interesting to note that a search in the CCDC database (updated Feb. 2017), shows up to 15 (for **1**) and 11 (for **2**) Ni^{II} dimers with similar triple-mixed bridges.[18,19] Only one of these compounds has been magnetically characterized which is similar bridge of **2**, and it show weak antiferromagnetic coupling ($J = -1.7\ cm^{-1}$).[20] Complex **1** is the first example and complex **2** is the second example of a Ni^{II} dimer containing triple-mixed μ-phenoxo, μ_2-η_2:η_1 acetate/end-on isothiocyanate and μ_2-1,3 *syn-syn* acetate bridges which have been magnetically characterized, and therefore, it is difficult to compare their magnetic properties with other similar complexes. Unfortunately, no correlation in magnetic properties of phenoxo/alkoxo/hydroxo and μ_2-η_2:η_1 acetate systems is known. But a number of correlations in diphenoxo/alkoxo/hydroxo-bridged systems have been reported. Binuclear nickel(II) complexes exhibit ferromagnetic or antiferromagnetic interactions is mainly related to the Ni–X–Ni bridging angle and twisting of the bridging moiety, favouring the orbital overlap between the Ni^{II} ions. There are two correlations for diphenoxo-bridged dinickel(II) compounds; if the Ni-$O_{phenoxo}$-Ni bridge angle is greater than 93.5° according to one[21] and 97.5° according to the other[22] antiferromagnetic behavior is expected. It has also been found that ferromagnetic exchange is reported in Ni-$N_{isothiocyanate}$-Ni bridged compounds when the bridge angle is less than 100°.[23,24] Since the Ni-$O_{phenoxo}$-Ni angle is 97.53° for **1** and 97.43° for **2**, which are greater than the crossover angles, the expected coupling through the first bridge should be antiferromagnetic for both complexes. Whereas, the Ni-$O_{\mu2\text{-}\eta2:\eta1\ acetate}$-Ni angle is 91.03° and the end-on isothiocyanate bridge angle is 89.05°, which are less than crossover angles, indicating that the expected magnetic coupling should be ferromagnetic through second bridge for both complexes. Thus, J values of different signs are expected for the two pathways. However, it is not possible to predict a priori which particular exchange pathway will be dominating. In addition, the third bridging group (μ_2-1,3 *syn-syn* acetate) is coordinated in axial-axial fashion to nickel(II) centers. While considering magnetic exchange interactions in hetero-bridged systems, the complementarity or counter complementarity effect of a second or third bridge on the first bridge should be taken into consideration.[25] It has been established that μ_2-1,3 *syn-syn* acetate moiety in hetero-bridged μ-phenoxo-μ_2-1,3 *syn-syn* acetate dicopper(II) systems exhibits a counter complementarity effect and thus reduces the antiferromagnetic interaction and the interaction in such systems becomes weakly antiferromagnetic and even ferromagnetic.[26] Moreover, the bridging moiety is not planar as evidenced by the torsion angle (19.19° for **1** and 15.45° for **2**) in the $[Ni_2O_2]$ unit and the dihedral angle (δ = 25.18° for **1** and 23.74° for **2**) between the two basal planes. When the dihedral angle decreases, both Ni–O–Ni and Ni–X–Ni bond angles also decrease. These lower bond angles, together with the worse overlap involving the in-plane orbitals of the bridges reduce the antiferromagnetic component of the coupling, and the experimental response is becoming small ferromagnetic for complex **1** or small antiferromagnetic for complex **2**.

Catecholase like activity of complexes 1 and 2

Both the two dinuclear Ni^{II} complexes demonstrated significant catalytic oxidation of 3,5-DTBC as monitored by means of UV–Vis spectroscopy. A blank experiment, carried out with only Ni^{2+} salt and 3,5-DTBC in the absence of the ligand and another blank experiment with only ligand and 3,5-DTBC in the absence of the Ni^{2+} salt, showed no band around ~400 nm in the UV–Vis spectra, suggesting the effectiveness of our complexes.

The kinetics for the oxidation of the substrate was determined by monitoring the increase of the product 3,5-

DTBQ, following the procedure reported in experimental section. The spectral scans for complex **1** and **2** are presented in Figure 4 and **S8**, respectively. Enzyme kinetics plots data for

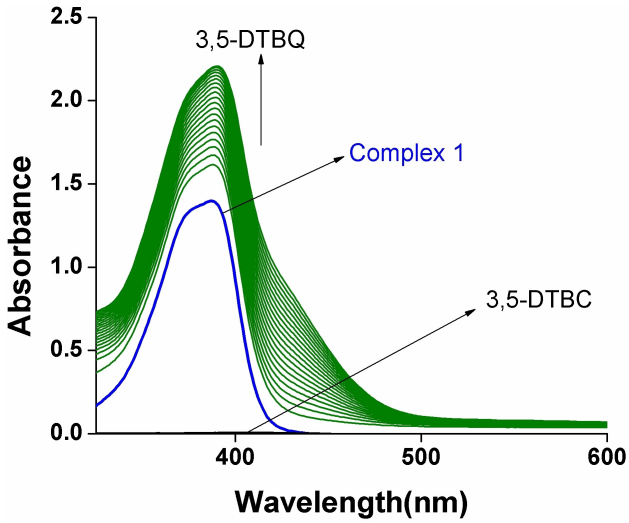

Figure 4. UV – Vis spectra of (i) complex **1**, (ii) 3,5-DTBC, and (iii) changes in UV – vis spectra of complex **1** upon addition of 3,5-DTBC (complex: 3,5-DTBC = 1: 50) observed after each 5 minutes interval.

complexes **1–2** are reported in **Figure S9–S12**. Analysis of the experimental data shows that the Michaelis binding constant (K_M) and V_{max} values are varying in a narrow range from 3.64×10^{-4} to 4.86×10^{-4} and 6.98×10^{-6} to 8.63×10^{-6}, respectively. Kinetic parameters for complexes **1–2** are shown in Table 2.

Table 2. Kinetic parameters of catecholase like activity for complexes **1–2**.

Catalyst	V_{max} (Ms^{-1})	K_M(M)	k_{cat}(h^{-1})
1	8.63×10^{-6}	3.64×10^{-4}	310.8
2	6.98×10^{-6}	4.86×10^{-4}	251.3

Table 3 represents the k_{cat} values of some previously reported dinuclear nickel complexes.[1d,10a,19,27–30] Upon comparison of Tables 2 and 3, it might be stated that our synthesized complexes belong to the highly efficient catalyst group, where the order of their activity is **1** > **2**. In order to get insight into the probable mechanism for the catecholase like activity cyclic volmatammetry, EPR and ESI-MS were performed.

Electrochemical experiments were performed for complexes **1–2** in methanolic solution. In the negative potential region, the complexes **1 — 2** exhibit two quasi reversible reduction waves at around ~ (−0.65 V) and ~ (−1.18 V) corresponding to $Ni^{II}Ni^{II}$/ $Ni^{II}Ni^{I}$ and $Ni^{II}Ni^{I}$/ $Ni^{I}Ni^{I}$ redox process (**Figure S13**).[2c,19] In the positive potential region both the complexes exhibit a quasi-reversible oxidative response around ~ +0.78 V (**Figure S14**). The observed redox process in this positive region can be assigned to the oxidation of Ni^{II} ion or thiocyanate ligand.[2c,11]

Table 3. k_{cat} values for catecholase like activity of different dinuclear nickel complexes.

Catalyst[a]	Solvent	k_{cat} (h^{-1})	Ref.[year]
1) $[Ni_2(L^1)_2(NCS)_2]$	Acetonitrile	64.1	28[2012]
2) $[Ni_2(LH_2)(H_2O)_2(OH)(NO_3)](NO_3)_3$	Methanol	14400	10a[2010]
3) $[Ni_2L(NO_3)(H_2O)_3]NO_3$	Methanol	1500	29[2012]
4) $[Ni_2(L^4)(SCN)_3(CH_3OH)_2]$	Methanol	161	19[2014]
5) $[Ni_2(L^2)(SCN)_2(AcO)(H_2O)]$	Methanol	863	19[2014]
6) $[Ni_2(HL^3)_4(H_2O)]$	Methanol	13800	27[2014]
7) $[Ni_2L_2(PhCOO)(H_2O)_2]ClO_4$	Methanol	167.64	1d[2016]
8) $[Ni_2L_2(NCS)(Ac)(H_2O)_{0.5}(MeOH)_{0.5}]$ $1.25H_2O$	DMF	10.08	30[2016]

[a]HL^1(1) = 2-[1-(3 methylaminopropylamino)-ethyl]phenol ; HL (2) = 2,6-bis (N-ethylpiperazine-iminomethyl)-4-methyl-phenol; H_2L(3) = N,N′-propylene-bis(3-formyl-5-tert-butylsalicylaldimine) ; HL^4(4) = 4-*tert*-Butyl-2,6-bis-[(2-pyridin-2-yl-ethylimino)-methyl]-phenol; HL^2(5) = 4-*tert*-Butyl-2,6-bis-[(2-di-methylamino-ethylimino)-methyl]-phenol;H_2L^3 (6) = 2-[(5-Hydroxy-pentylimino)-methyl]-4-methoxy-phenol. HL (7) = [(3-dimethylamino-propylamino)-methyl]-phenol; HL(8) = 2-((E)-(2-(pyridin-2-yl)ethylimino) methyl)-4-chlorophenol).

Figure S15 and **S16** depict the cyclic voltammogram of mixed solution of 3,5-DTBC with complex **1** and **2** in methanol, respectively. Both the voltammogram contain two reduction peaks at −0.86 to −0.90 V and −1.51 to −1.4 V. First redox response is obviously due to Ni^{II} reduction. Here two successive reduction of two Ni^{II} at −0.65 and −1.18 V might merge, giving only one reduction signal at −0.90 V. The second reduction at higher negative potential may be due reduction of the C=N bond of Schiff base ligand as reported previously.[19]

The reduction of ligand during the catechol oxidation is further proved by EPR experiment (**Figure S17**). Both the complexes are EPR silent as expected for octahedral Ni^{II} system. However, the mixture of 3,5-DTBC and complex **1** (as a representative) (50:1 ratio) gave a sharp EPR signal at $g\approx2$. This signal suggests the generation of organic radical which is responsible for oxidation process.[4a,19]

Spectroelectrochemical analysis of the complex **1** (as representative) and 3,5-DTBC mixture (1:50) in methanol at −1.51 V also suggests that the reduction of imine bond during the catalytic reaction is responsible for the oxidation of 3,5-DTBC (Figure 5**a**). Coulometric analysis of complex **1**(as representative) and 3,5-DTBC mixture (1:50) in methanol at −1.51 V and followed by the EPR experiments exhibits a sharp EPR signal at g = 2 also suggests the formation of an organic radical (Figure 5**b**).

The catalytic reaction performed under an inert atmosphere did not show the preparation of 3,5- DTBQ. However, the formation of 3,5-DTBQ was instantly noticed upon exposure of the reaction mixture to a dioxygen environment. It is now essential to know whether O_2 reduces to water or H_2O_2 during the catechol oxidation process. The oxidation of I^- to I_2 followed by the production of I_3^-, as is manifested from the UV – vis spectral study of the solution (**Figure S18**) obtained after proper workup of the mixture of catechol, complex, and KI (See Experimental Section), clearly indicates that O_2 is reduced to H_2O_2, as reported earlier.[4a]The formation of H_2O_2

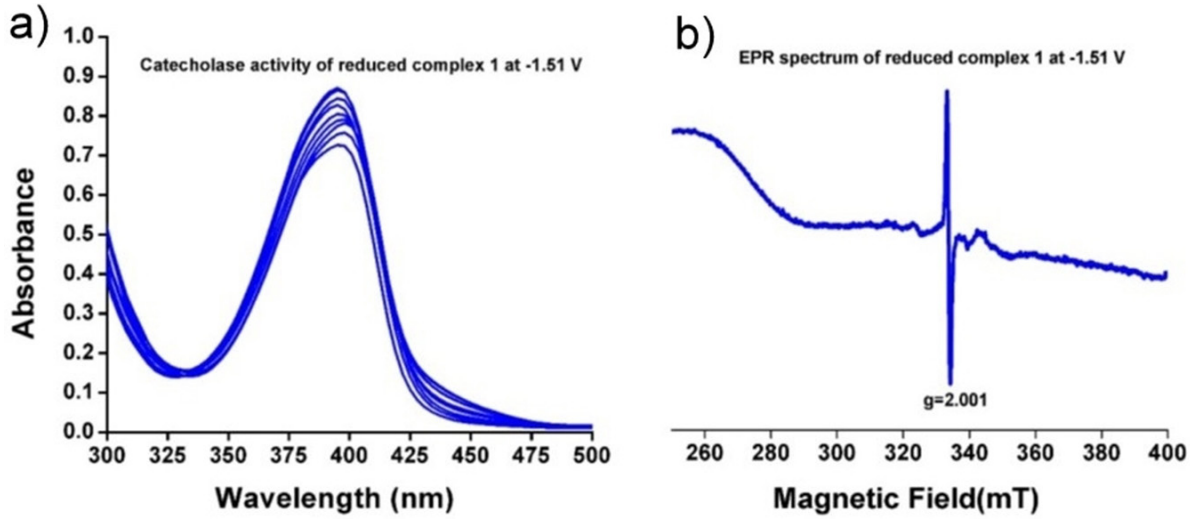

Figure 5. (a) Spectro-electrochemical graph of complex **1**(most active) at −1.5 V; (b) Coulometrically generate and spectroscopically (EPR) investigate the nature of the reduced species of complex **1** (most active).

was also verified separately in the absence of both oxygen and 3,5-DTBC. We did not find any indication for the generation of H_2O_2 in both the cases, implying that both the 3,5-DTBC and oxygen are required together for the generation of H_2O_2.

The electrospray ionization mass spectra (ESI-MS positive) of methanolic solutions of compounds **1–2** recorded are very similar. Each spectrum contains one major peak with the virtually the same line-to-line separations (to within one unit); m/z = 663.43 and 658.43 for **1** and **2**, respectively. These peaks, together with the isotopic distribution patterns, are assignable to the $[Ni_2^{II}(L^1)(CH_3COO)(SCN)]^+$, $[Ni_2^{II}(L^2)(CH_3COO)(SCN)]^+$, respectively (**Figure S19–20**).

To get an insight into the nature of the possible complex-substrate intermediate for catecholase like activity, ESI-MS positive spectra of a 1:50 mixture of the complexes with 3,5-DTBC were recorded after 2 min of mixing in methanol and the results are depicted in Figure 6 (for complex **1**) and **Figure S21** (For complex **2**). Both the spectra comprised of the peak that is found for the complex alone. In addition, one important peak for both the complexes observed at m/z = 825.31 and 820.36 are quite interesting because the peak positions clearly indicate that this peaks arise from the 1:1 complex–substrate aggregate $[Ni_2^{II}(L^1)(CH_3COO)(3,5\text{-}DTBC)]^+$ and $[Ni_2^{II}(L^2)(CH_3COO)(3,5\text{-}DTBC)]^+$ for complexes **1** and **2**, respectively, which are consistent with the rate saturation kinetics as discussed earlier. Inset picture of Figure 6 is representing the structure of the intermediate generated during catecholase like activity of complex **1** (as representative) in methanol. After 120 minutes the peak for the complex–substrate adduct for both complexes disappeared and one major peak along with the complex peak was appeared around at m/z = 243.14 can be assigned as $[3,5\text{-}DTBQ–Na]^+$, **Figure S22-23**. The presence of the complex peak in both the cases after catalytic process implies the regeneration of the catalyst.

The higher activity of complex **1** can be explained on basis of the higher effective charge on metal ion. Due to the presence of electronegative oxygen atom in the morpholine moiety, electron density may be dragged from nickel ion to oxygen which increases the positive charge on nickel ion in complex **1** than **2**. It is quite evident that the extra positive charge on the metal might be instrumental for higher catalyst–substrate interactions followed by higher efficiency for complex **1**. DFT calculations has been done to support this assumption (vide infra).

Another factor can also explain the order of the catecholase like activity. ESI-MS spectral study suggests that monodentate isothiocyante ligand was eliminated after the addition of 3,5-DTBC to both the complexes. Structural characterization reveals that Ni–N(NCS^-) bond distances are 2.04 and 2.02 Å for complexes **1** and **2**, respectively. A longer Ni–N bond distance for complex **1** causes easy dissociation to accommodate the incoming substrate 3,5-DTBC to a greater extent, thereby showing higher activity over complex **2**.

Discussions on computational calculations

As aforementioned, ESI-MS study reveals that the complex-substrate adduct for both catalysts have alike composition where two nickel centres are coordinated to corresponding Schiff base ligand, one acetate anion and one catecholate moiety. Nevertheless, complex **1** illustrates higher catecholase activity than complex **2**. We already revealed that the electron withdrawing effect of two electronegative oxygen atom present in the HL^1 ligand may increase the effective positive charge density on nickel centres in complex **1** and this higher positive charge on metals creates a channel to assist for the better catalyst–substrate interaction, a criterion for exhibiting better catalytic activity. We have performed a DFT calculation in order to substantiate this hypothesis. The most stable

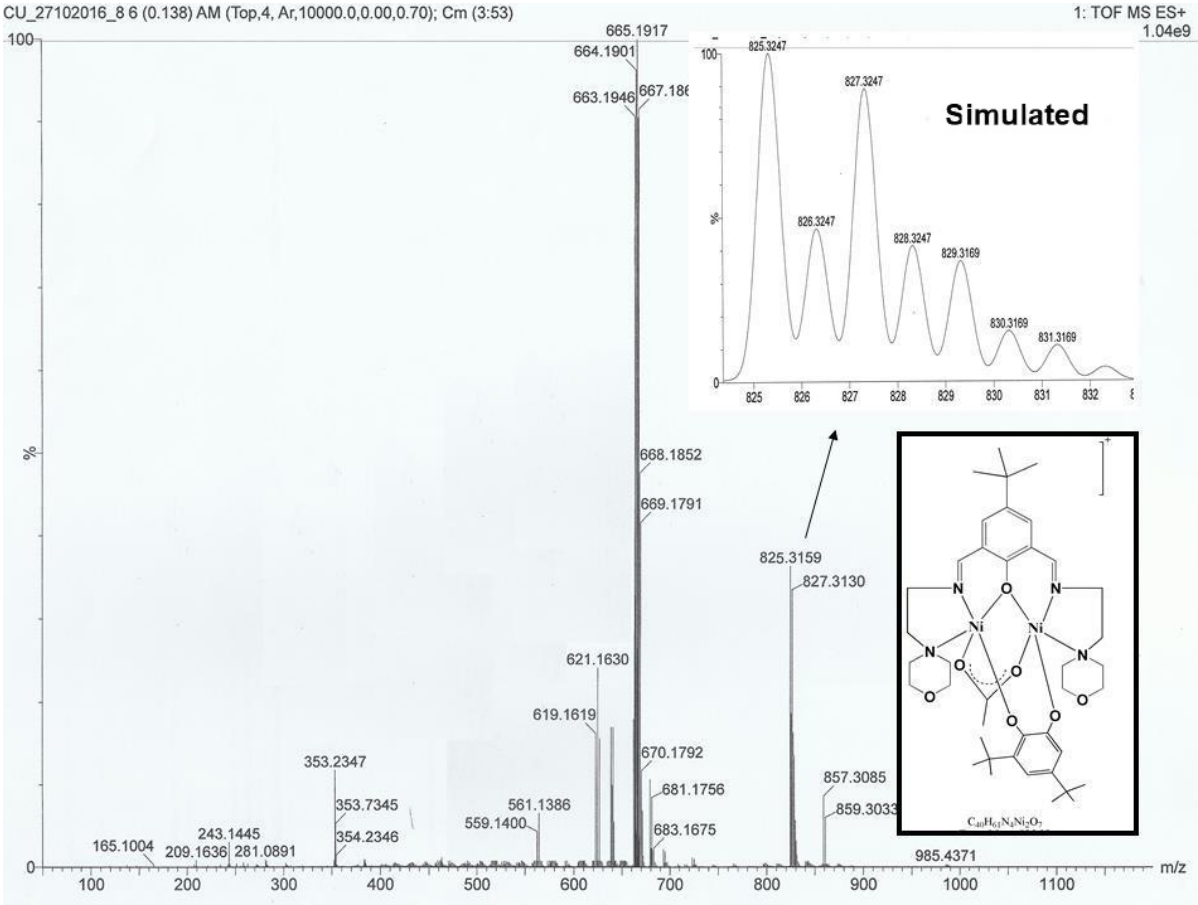

Figure 6. ESI-MS spectrum of 1: 100 mixtures of the complex **1** and 3,5-DTBC in methanol after 2 minutes of mixing. Inset: Structure of the probable species for the mixture of complex **1** and 3,5-DTBC (1:50) in methanol.

structures of modified **1** and **2** evidences to be open-shell quintet state (S = 2) with optimized structural parameters fully consistent with crystallographic data and the net spin on Ni^{II}. The partial charge on the nickel centres was calculated via Natural bond orbital (NBO) analysis. The results obtained from NBO analyses clearly suggest that the charge density on the metal is higher (+1.97) in complex **1** than that of in the complex **2** (+1.88). It undoubtedly supports our assumption that higher the effective charge on the metal ion higher will be the catalyst–substrate interactions followed by higher efficiency, as is observed in the case of complex **1**. Krebs and coworkers have proposed a similar kind of hypothesis where the catecholase activity of dinuclear copper complexes having different groups (-CH_2-/-O-/-S-) in the position 4 of the piperidine ring was investigated.[3] However, they proposed that the lability of one coordinated acetate ligand present in each catalyst increases from the catalyst with -CH_2- group to -S- group. Thus, the resulting unoccupied coordination site can be implemented for ease substrate binding, thereby resulting in higher efficiency towards the catechol oxidation for that complex with -S- group. In our case we propose the role of the auxiliary electronegative atom on catecholase activity in different aspect. In addition, DFT calculation reveals interesting difference between the two modified complex-catecholate adducts that could be also significant in describing the order of the catecholase activity (see Figure 7). Herein, catecholate is bounded to nickel centres via syn-syn didentate bridging mode in complex **1** whereas in complex **2** catecholate possess η^2:η^1 didentate bridging fashion.

The effect of catecholate binding mode on the rate of catecholase activity of Cu(II) complex system was reported by several groups.[31] However, only two examples have been found where η^2:η^1 didentate bridging fashion of catecholate moiety was proposed, and in those cases, they considered Cu(II) complex system.[32] η^2:η^1 didentate bridging fashion of catecholate moiety for Ni^{II} complex system has not been proposed till date. In the end, we can clearly conclude from theoretical calculations that complex-catecholate adduct with syn-syn bidentate bridging catecholate ion facilitate higher catecholase activity than that of the complex-catechol adduct consisting η^2: η^1 didentate bridging catecholate moiety.

Phosphatase like activity of complexes 1 and 2

The kinetics for the complexes **1–2** catalyzed hydrolysis of 4-NPP was determined by monitoring the increase of the product

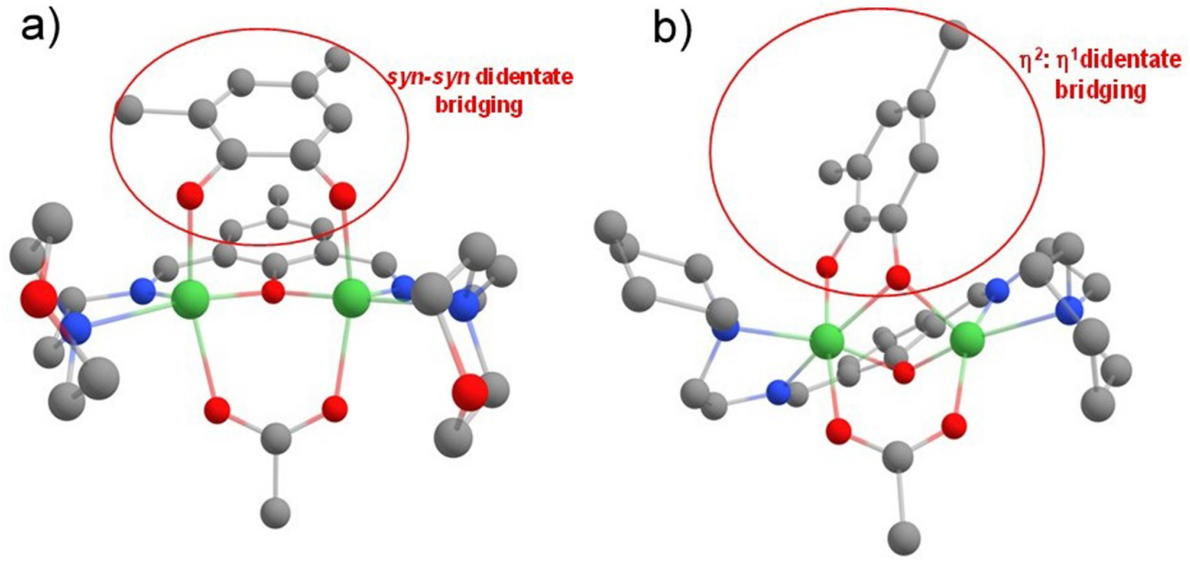

Figure 7. Optimized structures of (a) modified complex **1**-catecholate adduct and (b) modified complex **2**-catecholate adduct.

p-nitrophenolate ion following the procedure reported in experimental section. UV-Vis spectral change during the hydrolysis of 4-NPP by complex **1** is shown in Figure 8. UV-Vis

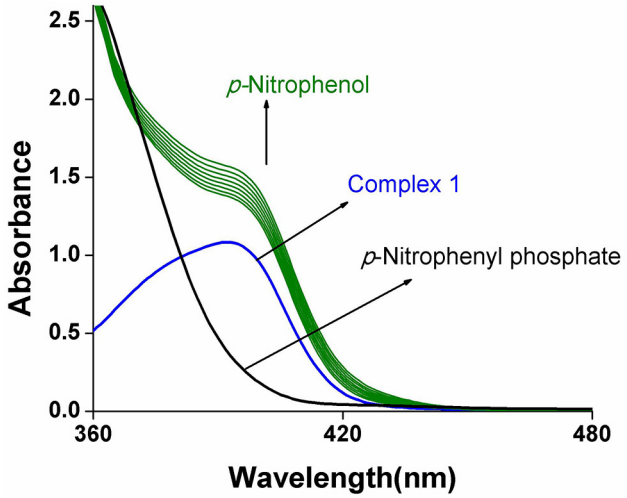

Figure 8. UV – Vis spectra of (i) complex **1**, (ii) 4-NPP, and (iii) changes in UV – Vis spectra of complex **1** upon addition of 4-NPP observed after each 5minute interval.

spectral change for **2** and kinetic plots for both the complexes are depicted in **Figure S24-S28**. Analysis of the experimental data yielded Michaelis binding constant (K_M) values are varying in a wide range from 7.11×10^{-4} to 1.38×10^{-3} whereas V_{max} values are varying comparatively in a narrow range from 2.59×10^{-6} to 4.04×10^{-6}. The turnover number (K_{cat}) values are obtained by dividing the V_{max} by the concentration of the catalyst, and are found to be 8.08×10^{-2} s^{-1} for complex **1** and 5.18×10^{-2} $s^{-1}$for complex **2**(Table 4). The spontaneous hydrol-

Table 4. Kinetic parameters of phoshatase like activity for complexes **1**–**2**.

Catalyst	V_{max} (Ms^{-1})	K_M(M)	k_{cat}(s^{-1})
1	4.04×10^{-6}	1.38×10^{-3}	8.08×10^{-2}
2	2.59×10^{-6}	7.11×10^{-4}	5.18×10^{-2}

ysis rate of 4-NPP was too low to be considered in the kinetic measurements. Thus, the general rate of spontaneous hydrolysis was not separately determined. Kinetic data for phosphatase like activities of previously reported dinuclear nickel complexes[2c,6b,7a,10a,11,13,33,34] are presented in Table 5. Comparing the Tables 4 and 5, it is evident that both the complexes **1** and **2** belong to high catalytically active group towards hydrolysis of 4-NPP and the activity is higher for **1**. Higher activity of the complex **1** towards phosphatase like activity can also be explained based on the high effective charge on metal ion as well as the lability of the counter anions as stated in catecholase like activity section.

Probable complex-substrate intermediate for phosphatase like activity has been also studied. ESI-MS positive spectra of a 1:50 mixture of the complexes with 4-NPP were recorded after 5 min of mixing in 97.5-2.5% MeOH-H_2O and the result for complex **1** are depicted in Figure 9. The spectrum contains two major peaks at m/z = 762.14 and 844.15 can be assigned as the 1:1 complex–substrate aggregate $[Ni_2^{II}(L^1)(4\text{-NPP})]^+$ and $[Ni_2^{II}(L^1)(CH_3COO)(4\text{-NPP})Na]^+$. The generation of these two intermediates clearly expresses that thiocyanate group eliminated first and followed by the acetate ion during phosphate activity. Rest of the peaks at m/z = 663.19 and 162.10 can be considered as molecular peak (vide supra) and sodium adduct of 4-nitrophenol, respectively. Similar observation was also found in complex **2** and the spectrum is shown in **Figure S29**. The experimental and the simulated spectral patterns are in

Table 5. Kinetic data for Phosphatase like activity of reported dinuclear nickel complexes along with the complexes **1–2**.

Catalyst[a]	Substrate[b]	Condition	$K_{PNPP}(S^{-1})$	Ref.[year]
1) $[Ni_2L^1(H_2O)_4]2ClO_4$	4-NPP	acetonitrile–water (2.5% (v/v)), pH 7.6,25 °C	1.85×10^{-2}	33[2010]
2) $[Ni_2(LH_2)(H_2O)_2(OH)(NO_3)](NO_3)_3$	4-NPP	methanol-water(1:1 v/v), 20 °C	2	10a[2010]
3) $[Ni_2(L^2)(L^3)(CH_3CN)]$	HPNP	30% DMF, pH 8.5,30 °C	8.73×10^{-3}	2c[2014]
4) $[Ni2(L^1)(O_2CMe)_2(H_2O)_2][PF_6]\cdot MeOH\cdot3H_2O$	HPNP	methanol–water (33% (v/v)), pH 8.5, 30 °C	14.7×10^{-4}	11[2009]
5) $[Ni_2(L2)(OAc)_2(CH_3CN)]BPh_4$	2,4-BDNPP	acetonitrile–water (50% (v/v)), pH 9,25 °C	386×10^{-3}	13[2008]
6) $[Ni_2L(\mu\text{-}OH)](ClO_4)_2$	BNPP	water-ethanol (1:1 v/v), pH 8.3, 25 °C	1.49×10^{-4}	34[2011]
7) $[Ni_2L_2(NCS)(Ac)(H_2O)_{0.5}(MeOH)_{0.5}]1.25H_2O$	4-NPP	DMF, 25 °C	8.17	6b[2016]
8) $[Ni_2L^1(\mu\text{-}NO_3)(NO_3)_2]$	4-NPP	DMSO, pH 5, 25 °C	6.66	7a[2016]

[a] (**1**) H_2L^1 = 12,25-Dimethyl-4,7,17,20-tetraoxa-3,8,16,21-tetraaza-tricyclo[21.3.1.110, 14]octacosa-1(26),2,8,10,12,14(28),15,21,23(27),24-decaene-27,28-diol; (**2**) HL = 2,6-bis(N-ethylpiperazine-iminomethyl)-4-methyl-phenol; (**3**)H_2L^2 = 1:2 schiff base of N^1-(2-Amino-ethyl)-ethane-1,2-diamine and 2-Hydroxy-5-nitro-benzaldehyde, H_2L^3 = 1:2 schiff base of N^1-Nitro-N^1(2-amino-ethyl)-propane-1,3-diamine and 2-Hydroxy-5-nitro-benzaldehyde ; (**4**) HL2 = 2-[N-(2-(pyridyl-2-yl) ethyl)(1-methylimidazol-2-yl)aminomethyl]-4-methyl-6-[N-(2-(imidazol-4-yl)ethyl)aminomethyl]phenol; (**5**) HL^1 = 2,6-Bis[N methyl-N-(2-pyridylethyl)- amino]-4-methylphenol; (**6**) HL = 2-{[(2-piperidylmethyl)amino]-methyl}-4-bromo-6-[(1-methylhomopiperazine-4-yl)methyl]phenol; (7) HL = 2-((E)-(2-(pyridin-2-yl)ethy-limino)methyl)-4-chlorophenol) ; (8) HL^1 = 4-Methyl-2,6-bis-{[methyl-(2-pyridin-2-yl-ethyl)-amino]-methyl}-phenol.

[b] 4-NPP = 4-nitrophenylphosphate; HPNP = 2-hydroxypropyl-p-nitropenylphosphate; 2,4-BDNPP = bis(2,4-dinitrophenyl)phosphate;BNPP = bis(4-nitrophenyl) phosphate.

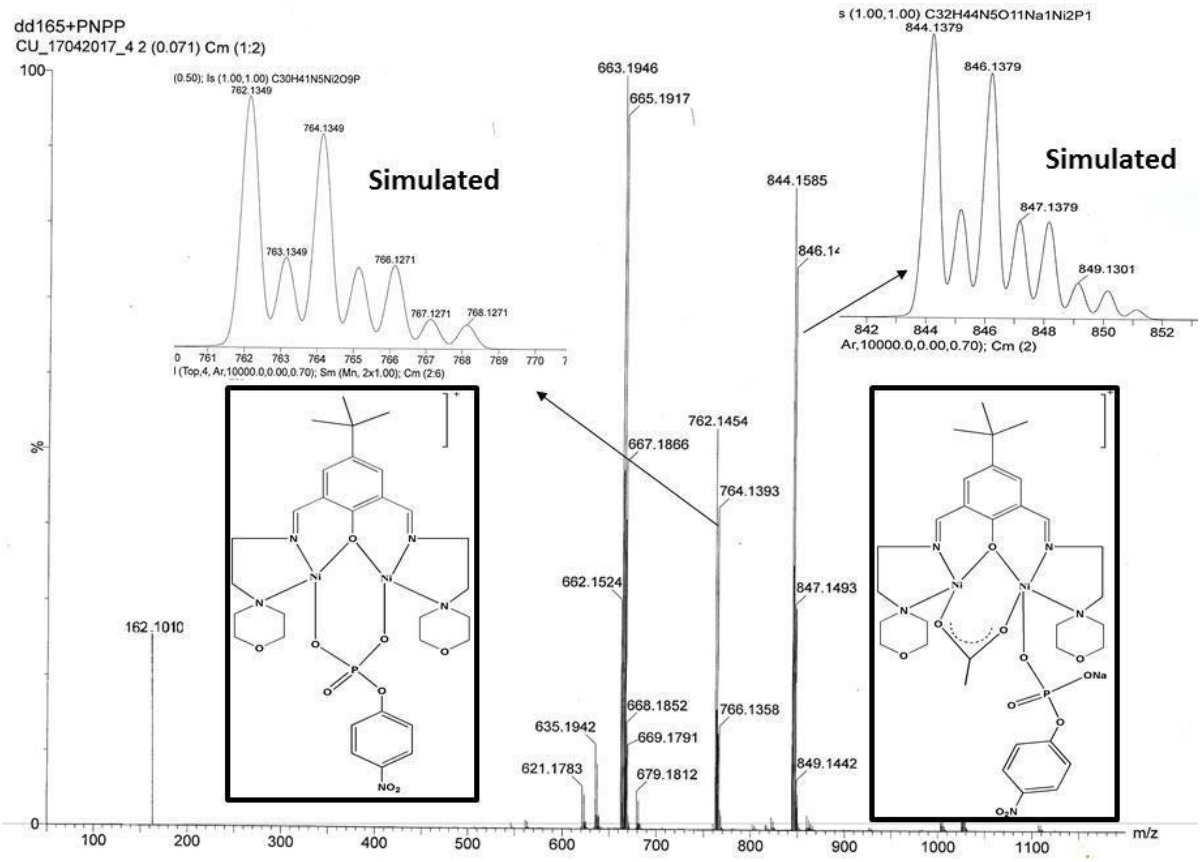

Figure 9. ESI-MS spectrum of 1: 50 mixtures of the complex **1** and 4-NPP in 97.5-2.5% MeOH-H_2O after 5 minutes of mixing. Inset: Structure of the two probable intermediate species for the mixture of complex **1** and 4-NPP (1:50) in methanol-water.

excellent agreement with each other, indicating right assignment of the species.

Conclusions

Triple-mixed phenoxo and acetato/isothiocyanato bridged two dinulcear nickel complexes of two slightly different end off compartmental ligands HL^1 and HL^2, namely 2,6-bis((*E*)-(2-morpholinoethylimino)methyl)-4-tert-butylphenol and 2,6-bis ((*E*)-(2-(piperidin-1-yl)ethylimino)methyl)-4-tert-butylphenol, have been purposely synthesized to inspect the role of the auxiliary electronegative atom present in nickel Schiff base compound on catecholase and phosphatase like activities. And finally, from experimental investigations along with theoretical

support we are able to conclude that presence of electronegative auxiliary atom in ligand moiety along with the substrate binging mode have substantial influence on both these bio activities. Syn-syn didentate and $\eta^2:\eta^1$ didentate bridging fashion of catecholate moiety in dinuclear Ni^{II} complex catalysed catecholase activity have been proposed where well-known syn-syn didentate catecholate bridging encourages for higher catecholase activity than that of the unprecedented $\eta^2:\eta^1$ didentate bridging mode of catecholate moiety.

Supporting information summary

Supplementary information includes FT-IR spectra, electronic spectra, kinetic plots, cyclic voltammograms, EPR, ESI-MS spectra and DFT data. It also contains experimental section of this paper. CCDC numbers 1041169–1041170 (complexes 1–2) contain supplementary crystallographic data for this article.

Conflict of Interest

The authors declare no conflict of interest.

Keywords: Catecholase-like activity · Mechanistic study · Nickel (II) complex · Phosphatase-like activity

[1] a) N. Mitic, Smith, J. S. A. Neves, L. W. Guddat, L. R. Gahan, G. Schenk, *Chem. Rev.* **2006**, *106*, 3338; b) M. G. Gichinga, S. Striegler, *J. Am. Chem. Soc.* **2008**, *130*, 5150; c) N. A. Rey, A. Neves, A. J. Bortoluzzi, C. T. Pich, H. Terenzi, *Inorg. Chem.* **2007**, *46*, 348; d) M. Mondal, P. M. Guha, S. Giri, A. Ghosh, *J. Mol. Catal. A: Chem.* **2016**, *424*, 54; e) R. E. H. M. B. Osorio, R. A. Peralta, A. J. Bortoluzzi, V. R. de Almeida, B. Szpoganicz, F. L. Fischer, H. Terenzi, A. S. Mangrich, K. M. Mantovani, D. E. C. Ferreira, W. R. Rocha, W. Haase, Z. Tomkowicz, A. dos Anjos, A. Neves, *Inorg. Chem.* **2012**, *51*, 1569; f) L. R. Gahan, S. Smith, A. Neves, G. Schenk, *Eur. J. Inorg. Chem.* **2009**, 2745; g) A. Neves, M. Lanznaster, A. Bortoluzzi, R. A. Peralta, A. Casellato, E. E. Castellano, P. Herrald, M. J. Riley, G. Schenk, *J. Am. Chem. Soc.* **2007**, *129*, 7486.

[2] a) P. Zerón, M. Westphal, P. Comba, M. Flores-Álamo, A. C. Stueckl, C. Leal-Cervantes, V. M. Ugalde-Saldívar, L. Gasque, *Eur. J. Inorg. Chem.* **2017**, 56; b) R. Sanyal, P. Kundu, E. Rychagova, G. Zhigulin, S. Ketkov, B. Ghosh, S. K. Chattopadhyay, E. Zangrando, D. Das, *New. J. Chem.* **2016**, *40*, 6623; c) V. K. Bhardwaj, A. Singh, *Inorg. Chem.* **2014**, *53*, 10731; d) S. K. Dey, A. Mukherjee, *New. J. Chem.* **2014**, *38*, 4985.

[3] M. Merkel, N. Mçller, M. Piacenza, S. Grimme, A. Rompel, B. Krebs, *Chem. Eur. J.* **2005**, *11*, 1201.

[4] a) J. Adhikary, P. Chakraborty, S. Das, T. Chattopadhyay, A. Bauzá, S. K. Chattopadhyay, B. Ghosh, F. A. Mautner, A. Frontera, D. Das, *Inorg. Chem.* **2013**, *52*, 13442; b) R. Sanyal, A. Guha, T. Ghosh, T. K. Mondal, E. Zangrando, D. Das, *Inorg. Chem.* **2014**, *53*, 85.

[5] a) J. Adhikary, A. Chakraborty, S. Dasgupta, S. K. Chattopadhyay, R. Kruszynski, A. Trzesowska-Kruszynska, S. Stepanović, M. Gruden-Pavlović, M. Swart, D. Das, *Dalton Trans.* **2016**, *45*, 12409; b) M. J. Gajewska, W. Ching, Y. Wen, C. Hung, *Dalton Trans.* **2014**, *43*,14726; c) M. Shyamal, T. K. Mandal, A. Panja, A. Saha, *RSC Adv.* **2014**, *4*, 53520.

[6] a) S. Dasgupta, I. Majumder, P. Chakraborty, E. Zangrando, A. Bauza, A. Frontera, D. Das, *Eur. J. Inorg. Chem.* **2017**, 133; b) R. Sanyal, X. Zhang, P. Chakraborty, S. Giri, S. K. Chattopadhyay, C. Zhao, D. Das, *New J. Chem.* **2016**, *40*, 7388.

[7] a) R. Sanyal, X. Zhang, P. Chakraborty, F. A. Mautner, C. Zhao, D. Das, *RSC Adv.* **2016**, *6*, 73534; b) P. Chakraborty, J. Adhikary, B. Ghosh, R. Sanyal, S. K. Chattopadhyay, A. Bauza, A. Frontera, E. Zangrando, D. Das, *Inorg. Chem.* **2014**, *53*, 8257.

[8] J. Adhikary, P. Chakraborty, S. Samanta, E. Zangrando, S. Ghosh, D. Das, *Spectrochim. Acta, Part A* **2017**, *178*, 114.

[9] I. Majumder, P. Chakraborty, J. Adhikary, H. Kara, E. Zangrando, A. Bauza, A. Frontera, D. Das, *ChemistrySelect* **2016**, *3*, 615.

[10] a) T. Chattopadhyay, M. Mukherjee, A. Mondal, P. Maiti, A. Banerjee, K. S. Banu, S. Bhattacharya, B. Roy, D. J. Chattopadhyay, T. K. Mondal, M. Nethaji, E. Zangrando, D. Das, *Inorg. Chem.* **2010**, *49*, 3121; b) A. Guha, K. S. Banu, S. Das, T. Chattopadhyay, R. Sanyal, E. Zangrando, D. Das, *Polyhedron* **2013**, *52*, 669.

[11] S. Mandal, V. Balamurugan, F. Lloret, R, Mukherjee, *Inorg. Chem.* **2009**, *48*, 7544.

[12] E. Monzani, L. Quinti, A. Perotti, L. Casella, M. Gullotti, L. Randaccio, S. Geremia, G. Nardin, P. Faleschini, G. Tabbi, *Inorg. Chem.* **1998**, *37*, 553.

[13] A. Greatti, M. Scarpellini, R. Peralta, A. Casellato, A. J. Bortoluzzi, F. R. Xavier, R. Jovito, M. A. De Brito, B. Szpoganicz, Z. Tomkowicz, M. Rams, W. Haase, A. Neves, *Inorg. Chem.* **2008**, *47*, 1107.

[14] L. Botana, J. Ruiz, A. J. Mota, A. Rodríguez-Diéguez, J. M. Seco, I. Oyarzabal, E. Colacio, *Dalton Trans.* **2014**, *43*, 13509.

[15] J.-E. Jee, C.-H. Kwak, *Inorg. Chem. Commun.* **2013**, *33*, 95.

[16] R. Biswas, S. Mukherjee, S. Ghosh, C. Diaz, A. Ghosh, *Inorg. Chem. Commun.* **2015**, *56*, 108.

[17] J. Kühnert, T. Rüffer, P. Ecorchard, B. Bräuer, Y. Lan, K. Powell, H. Lang, *Dalton Trans.* **2009**, *23*, 4499.

[18] H. Adams, S. Clunas, D. E. Fenton, S. E. Spey, *J. Chem. Soc. Dalton. Trans.* **2002**, 441.

[19] T. Ghosh, J. Adhikary, P. Chakraborty, P. K. Sukul, M. S. Jana, T. K. Mondal, E. Zangrando, D. Das, *Dalton. Trans.* **2014**, *43*, 841.

[20] T. Koga, H. Furutachi, T. Nakamura, N. Fukita, M. Ohba, K. Takahashi, H. Okawa, *Inorg. Chem.* **1998**, *37*, 989.

[21] K. K. Nanda, L. K. Thompson, J. N. Bridson, K. Nag, *J. Chem. Soc., Chem. Commun.* **1994**, 1337.

[22] X.-H. Bu, M. Du, L. Zhang, D.-Z. Liao, J.-K. Tang, R.-H. Zhang, M. Shionoya, *Dalton Trans.* **2001**, 593.

[23] A. Donmez, G. Oylumluoglu, M. B. Coban, C. Kocak, M. Aygun, H. Kara, *J. Mol.Struc.* **2017**, *1149*, 569.

[24] M. G. Barandika, R. Cortés, Z. Serna, L. Lezama, T. Rojo, M. K. Urtiaga, M. I. Arriortua, *Chem. Commun.* **2001**, 45.

[25] S. Hazra, R. Koner, P. Lemoine, E. C. Sañudo, S. Mohanta, *Eur. J. Inorg. Chem.* **2009**, 3458–3466.

[26] O. Kahn, Molecular Magnetism, VCH Publications, New York, **1993**.

[27] R. Modak, Y. Sikdar, S. Mandal, S. Chatterjee, A. Bieńko, J. Mroziński, S. Goswami, *Inorg. Chim. Acta* **2014**, *416*, 122.

[28] A. Biswas, L. K Das, M. G. B. Drew, G. Aromí, P. Gamez, A. Ghosh, *Inorg. Chem.* **2012**, *51*, 7993.

[29] S. Das, P. Maiti, T. Ghosh, E. Zangrando, D. Das, *Inorg. Chem. Commun.* **2012**, *15*, 266.

[30] R. Sanyal, S. K. Dash, P. Kundu, D. Mandal, S. Roy, D. Das, *Inorg. Chim. Acta* **2016**, *453*, 394.

[31] a) H. Börzel, P. Comba, H. Pritzkow, *Chem. Commun.* **2001**, 97; b) A. Granata, E. Monzani, L. Casella, *J. Biol. Inorg. Chem.* **2004**, *9*, 903; c) S. Torelli, C. Belle, S. Hamman, J. Pierre, *Inorg. Chem.* **2002**, *41*, 3983; d) J. Ackermann, F. Meyer, E. Kaifer, H. Pritzkow, *Chem. Eur. J.* **2002**, *8*, 247; e) A. Szorcsik, F. Matyuska, A. Bényei, N. V. Nagy, R. K. Szilágyie, T. Gajda, *Dalton Trans.* **2016**, *45*, 14998.

[32] a) T. Plenge, R. Dillinger, L. Santagostini, L. Casella, F. Tuczek, *Z. Anorg. Allg. Chem.* **2003**, *629*, 2258; b) E. Peyroux, W. Ghattas, R. Hardré, M. Giorgi, B. Faure, A. J. Simaan, C. Belle, M. Réglier, *Inorg. Chem.* **2009**, *48*, 10874.

[33] S. Anbu, M. Kandaswamy, B. Varghese, *Dalton Trans.* **2010**, *39*, 3823.

[34] Y. Ren, J. Lu, B. Cai, D. Shi, H. Jiang, J. Chen, D. Zheng, B. Liu, *Dalton Trans.* **2011**, *40*, 1372.

Submitted: November 27, 2017
Revised: January 18, 2018
Accepted: January 19, 2018